COBEM2015

ABCM Associação Brasileira de Engenharia e Ciências Mecânicas

23rd ABCM International Congress of Mechanical Engineering
December 6-11, 2015, Rio de Janeiro, RJ, Brazil

EXPERIMENTAL DESIGN OF ROBUST CONTROLLER FOR A RIGID FLEXIBLE SATELLITE

Luiz Carlos Gadelha de Souza
University of Brasília – UnB- Campus Gama - FGA, 72405-610, Brasília-DF
lcgadelha@gmail.com

Breno Braga Galvão
University of Brasília – UnB - Campus Gama - FGA, 72405-610, Brasília-DF
breno.braga.galvao@gmail.com

Abstract. *Future space missions with flexible structures like robotic manipulators; solar sail and satellite with large panels and/or antennas will need great performance and robustness of the Attitude Control Systems (ACS) algorithms. Major limiting factors of that control system are the unwanted vibrations of the flexible parts after big manoeuvres in space. As a result, an active ACS must be used to compensate and/or to damp out the remaining flexible vibrations. On the other hand, one way to increase reliability and reduce cost of the ACS project is using experimental platforms and prototypes to simulate space conditions. Experimental test has the advantage of introducing more realism than the computer simulation, although, it has the difficulty of reproducing zero gravity and torque free space condition. In this paper one studies the dynamics and the control system of a rigid flexible beam using the Quanser Rotary Flexible Link System. The dynamics is investigated by two mathematical models. The first one is developed using the single mass-spring approach and the second one using the assumed modes method. The control system is designed using the traditional LQR (Linear Quadratic Regulator) technique. Although the LQR is very well know, a first important objective of this study is to highlight the advantages and benefits of using experimentally the LQR approach as for control algorithm development aiming at a flexible satellite on board computer implementation. The second is to compare the LQR controller performance and robustness when it is designed using the mass-spring model and the assumed modes model.*

Keywords: *Robust control system, Rigid-flexible satellite.*

1. INTRODUCTION

There are several methodologies (Hall et al, 2002) to design satellite ACS, depending on the control system complexity; computer simulation cannot be the more appropriate one. Experimental platforms (Schwartz et al, 2003) have the important advantage of allowing the satellite dynamics representation in laboratory to accomplish experiments and simulations to evaluate satellites ACS. Experimental test has also the possibility of introducing more realism than the simulation; but it has the difficulty of reproducing zero gravity and torque free space condition. Examples of simulator dynamics and control system experimental investigations can be found in (Conti and Souza, 2008 ; Souza and Gonzales, 2012). A classic case of a phenomenon that was not investigated experimentally before launch, was the dissipation energy effect that has altered the satellite Explorer I rotation (Kaplan, 1976). Several institutions and universities (Tsiotras, 2007; Sales, et.al, 2013) are investigating and testing the ACS performance by experimental prototypes. In (Barbosa and Goes, 2007 ; Souza and Souza, 2015 ; Bigot and Souza, 2014) it was showed that the influence of the non-linearities introduced by the slosh motion, the panel's flexibility and the system parameters variation can degrade the control system performance, indicating the necessity of new robust control technique. Examples of multi-objectives methods to design controllers space system can be found in (Mainenti-Lopes, et. al, 2012; Pinheiro and Souza, 2013) application In this paper one investigates and compares the LQR controller robustness and performance when it is designed for two different rigid-flexible satellite models represented by the Rotary flexible link module which consist of a rigid central hub connected to a flexible appendage (Quanser, homepage). The two mathematical models are obtained by the Lagrangian formulation where the first model uses a Mass Spring Model (MSM) configuration to describe the rigid-flexible dynamics and the second one uses the Distributed Parameters Model (DPM) based on assumed modes method to describe the various vibration modes of the system. The model dynamics analyse has shown that although both models are obtained by different approach, the two models are representative of the rigid-flexible system and they are useful to be used in the LQR controller design. As for the controller performance and robustness one observes that the LQR technique is much appropriated, the only weakness is the fact that one assumes that all the states are available which is not always true.

2. EXPERIMENTAL SETUP

The Quanser flexible link setup is showed in Figure 1. The LQR controller's performances are investigated by simulation for the MSM and DPM, which performance criterion are to control rigid motion and damp the flexible displacement as quick as possible. The outputs measurements are the angular and flexible displacement and their variation on time. One knows that the flexible link is subject to noises due to sensors and actuator dynamics and due to no modeled dynamics. However, in this investigation these perturbations are disregards.

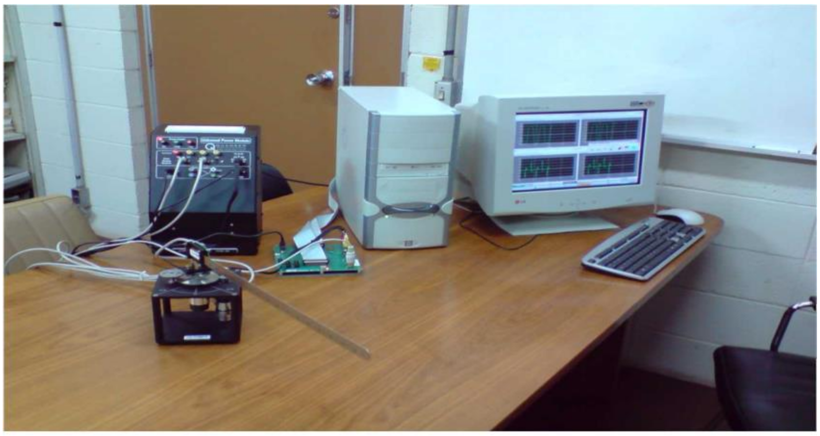

Figure 1: Complete Quanser flexible link set up used to derive the DPM and MSM models

3. FLEXIBLE BEAM MODEL

Figure 2 shows the behavior of the Rotary flexible link module rotation where the rigid angular displacement is θ and the flexible displacement is y (t, L), L is the length of the beam, J_b and r are the inertia moment and the radius of the hub, respectively.

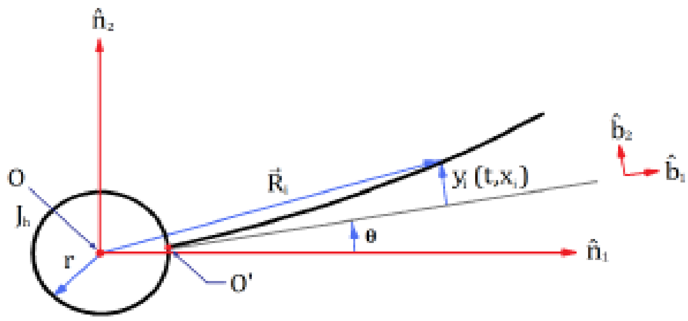

Figure 2: Rigid flexible beam rotation

3.1 Mass Spring Model

The equations of motion of MSM is obtained considering the rigid flexible beam represented by fig. 3

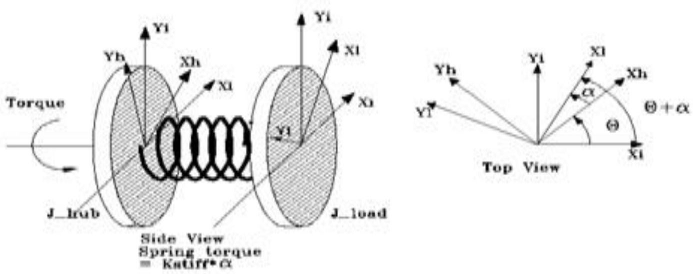

Figure 3: Flexible link represented by Mass Spring Model.

The rotary spring equations of motion is given by

$$J\,\ddot{\alpha} = -K\alpha \tag{1}$$

where J and K are inertia and the link stiffness that is related to the angle α and the link's damped natural frequency by

$$\ddot{\alpha} = -\omega_c^2 \alpha \tag{2}$$

Combining equations (1) and (2), one obtains

$$K = \omega_c^2 J \tag{3}$$

Using the Lagrange formulation one needs the Kinetic and Potential energies of the system which given by

$$L = T - V = \frac{J_{eq}\dot{\theta}^2}{2} + \frac{J\left(\dot{\theta}+\dot{\alpha}\right)^2}{2} - \frac{K\alpha^2}{2} \tag{4}$$

Using two generalized coordinates the rigid angle θ and the flexible displacement α the solution of the Lagrange equation results in two equations of motions given by

$$J_{eq}\ddot{\theta} + J_{ARM}\left(\ddot{\theta}+\ddot{\alpha}\right) = T_{OUTPUT} - B_{eq}\dot{\theta} \tag{5}$$

$$J_{ARM}\left(\dot{\theta}+\dot{\alpha}\right) + K\alpha = 0 \tag{6}$$

The output torque on the load from the motor is given by

$$T_{OUTPUT} = \frac{\eta_m \eta_g K_T K_g (V_m - K_g K_m)\dot{\theta}}{R_m} \tag{7}$$

Combining equations (5), (6) and (7), one obtains the state-space equations of motion of the system given by

$$\begin{bmatrix}\dot{\theta}\\ \dot{\alpha}\\ \ddot{\theta}\\ \ddot{\alpha}\end{bmatrix} = \begin{bmatrix} 0 & 0 & 1 & 0\\ 0 & 0 & 0 & 1\\ 0 & \dfrac{K}{J_{eq}} & \dfrac{-\eta_m\eta_g K_T K_m K_g^2 + B_{eq}R_m}{J_{eq}R_m} & 0\\ 0 & \dfrac{-K\left(J_{eq}+J_{ARM}\right)}{J_{eq}J_{ARM}} & \dfrac{\eta_m\eta_g K_T K_m K_g^2 + B_{eq}R_m}{J_{eq}R_m} & 0 \end{bmatrix} \begin{bmatrix}\theta\\ \alpha\\ \dot{\theta}\\ \dot{\alpha}\end{bmatrix} + \begin{bmatrix} 0\\ 0\\ \dfrac{\eta_m\eta_g K_T K_g}{J_{eq}R_m}\\ \dfrac{-\eta_m\eta_g K_T K_g}{J_{eq}R_m}\end{bmatrix} V_m \tag{8}$$

where η_m and η_g are the motor and gearbox efficiencies, K_T and K_g are transmission and motor ration. R_m is the armature resistance, V_m the armature input voltage, K_m the back-emf constant and J_{eq} the equivalent moment of inertia at the load.

3.2 Distributed Parameters Model

The Distributed Parameters Model (DPM) is obtained considering the flexible displacement represented by y (t, x) as showed in fig. 2 from which the position vector R of any point on the deformed beam is given by

$$\vec{R} = (r+x)\widehat{b}_1 + y\widehat{b}_2 \tag{9}$$

Like before using the Lagrange formalism one needs the Kinetic energy of the system given by

$$T = 1/2\hat{J}\dot{\theta}^2 + 1/2\int_0^L \rho\dot{y}^2 dx + \int_0^L \rho\dot{y}(r+x)dx \tag{10}$$

$$where \qquad \widehat{J} = J_{hub} + \int_0^L \rho(r+x)^2 dx$$

and the potential energy given by

$$V = 1/2\int_0^L EI(y''(t,x))^2 dx \tag{11}$$

Using the assumed modes method where the elastic modes are modelled as

$$y(x,t) = \sum_{j=1}^{N} q_j(t)\phi_j(x) \tag{12}$$

where $q_j(t)$ is the generalized coordinates representing the flexibility , N is the modes numbers and $\phi_j(x)$ are the shape functions given by

$$\phi_j(x) = 1\text{- }\cos\left(\frac{j\pi x}{L}\right) + \frac{1}{2}(\text{-}1)^{j+1}\left(\frac{j\pi x}{L}\right)^2 \tag{13}$$

Substituting the eqs 13 and 12 into eqs 11 and 10 the total kinetic and potential energies are

$$\text{T} = \frac{1}{2}\hat{J}\,\dot{\theta}^2 + \frac{1}{2}\sum_{j=1}^{N}\dot{q}^2{}_j(t)\int_0^L \rho\phi_j(x)q_k(x)dx + \dot{\theta}\sum_{j=1}^{N}\dot{q}^2{}_j(t)\int_0^L \rho(r+x)\phi_j(x)dx \tag{14}$$

$$\text{V} = \frac{1}{2}\sum_{j=1}^{N}\dot{q}^2{}_j(t)\int_0^L EI\phi_j''(x)\phi''_k(x)dx \tag{15}$$

Taking into account the two generalized coordinates θ and $q_j(t)$ the solution of the Lagrange equation results in two equations of motions given by

$$2\hat{J}\ddot{\theta}\sum_{j=1}^{N}\ddot{q}_j\int_0^L \rho(r+x)\phi_j(x)dx = u \tag{16}$$

$$\sum_{j=1}^{N}\ddot{q}_j(t)\int_0^L \rho\phi_j(x)\phi_k(x)dx + \ddot{\theta}\sum_{j=1}^{N}\int_0^L \rho(r+x)\phi_j(x)dx + \sum_{j=1}^{N}q_j(t)\int_0^L EI\phi_j''(x)\phi_k''(x)dx = 0 \tag{17}$$

Assuming

$$\lfloor M_{\theta q}\rfloor_j = \int_0^L \rho(r+x)\phi_j(x)dx$$

$$\lfloor M_{qq}\rfloor_{jk} = \int_0^L \rho\phi_j(x)\phi_k(x)dx$$

$$\lfloor K_{qq}\rfloor_{k} = \int_0^L EI\phi_j''(x)\phi''_k(x)dx$$

The DC control input u and the motor torque T_m are given by

$$u = T_m - B_{eq}\dot{\theta} \tag{18}$$

$$T_m = \frac{\eta_m\eta_g K_T K_g(V_m - K_g K_m\dot{\theta})}{R_m} \tag{19}$$

where $C_m = \dfrac{\eta_m \eta_g K_T K_g}{R_m}$

The controller u can be write as

$$u = C_m V - (C_m K_g K + B_{eq})\dot{\theta} \tag{20}$$

As a result, the last equations in matrix form is

$$\dot{x} = \begin{bmatrix} J & M^T{}_{\theta q} \\ M^T{}_{\theta q} & M_{qq} \end{bmatrix} x + \begin{bmatrix} C_m K_g + B_{eq} & 0 \\ 0 & 0 \end{bmatrix} x + \begin{bmatrix} 0 & 0 \\ 0 & K_{qq} \end{bmatrix} x - \begin{bmatrix} C_m \\ 0 \end{bmatrix} u \tag{21}$$

where $x = (\theta, \alpha, \dot{\theta}, \dot{\alpha})$

4. OPEN LOOP MODELS ANALYSE

Before starting the design of controllers it should be interesting to analyse the dynamic behaviour of both models, since by this analysis it is 'possible to foresee the difficulties that both models can impose in the controller design. Figures 4 and 5 show the singular values for both models, from which is possible to observe that there is reasonable difference between the singular values behaviour. The reason for that is because each model is obtained by different modelling techniques, resulting in different matrices A, B and C. It is known that the MSM technique is very imprecise and it should be applied just for simple model, meanwhile DSM modelling technique is more complicated to be applied, since it take into account the discretization of the system.

The advantage is the possibility of obtaining a more accurate model which is closer to the reality. Another problem that must be observed is the location of the sensors and actuators; because both models deal with the flexibility dynamics which in realistic terms present a serious difficult to know where is the best place to put the sensor and the actuator. To put sensor and actuator over the flexible part of the system is a complicate matter; see (Souza, 2015) for more details.

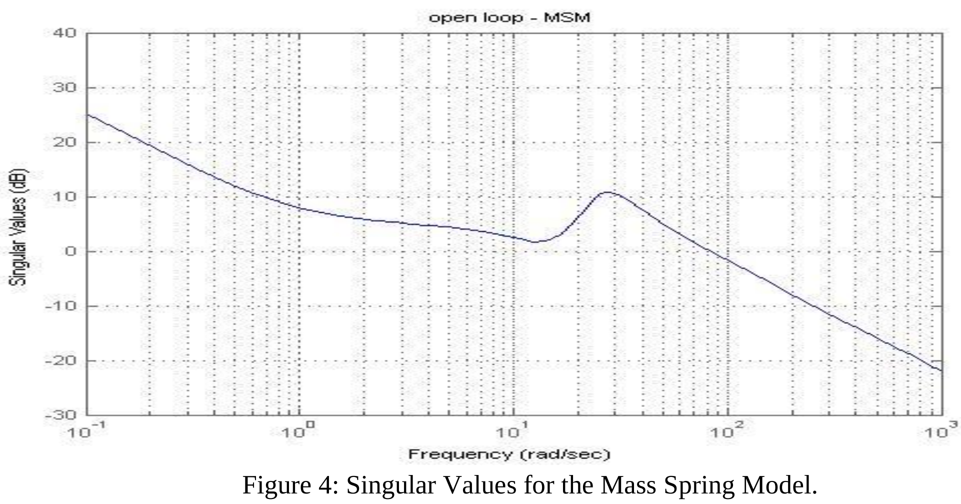

Figure 4: Singular Values for the Mass Spring Model.

Although the singular values of both models have differences behaviour, it should point out that both models represents the same dynamic. From the peak in fig. 5 it is evident is that the DPM model represents the dapping of the system mode accurate than the MSM model. Apart from that it is expected that as for the design of the LQR controller this difference will not introduces major problems.

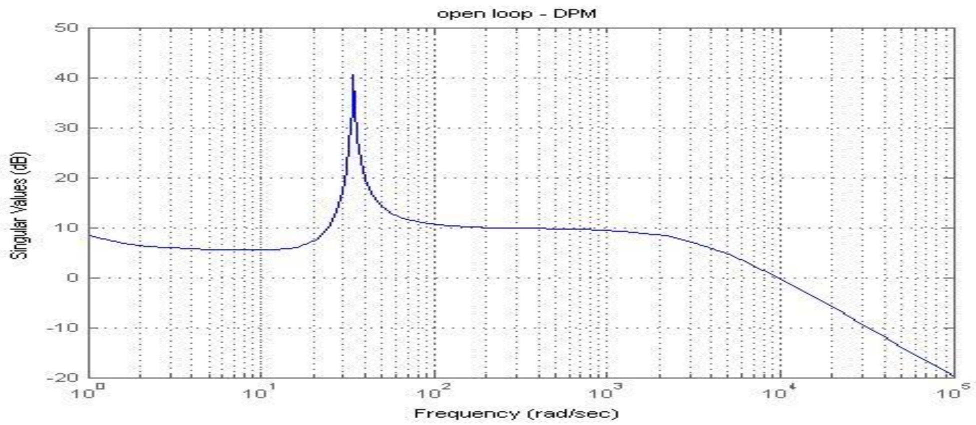

Figure 5: Singular values for the Distributed Parameters Model.

5. SIMULATIONS RESULTS

The LQR controller performance and robustness has been investigated developing a Matlab/Simulink program of the complete system, where the both MSM and DPM model have one control input and four states to be controlled. After some trial and error tuning the weight matrix Q, the best value obtained is Q = diag (400, 10000, 3, 2) with R = 1.

Figures 6 and 7 shows the LQR controller performance controlling the angular and flexible displacement, when it is designed using the MSM and the DPM models. Figures 6 and 7 also show the LQR Mix controller performance controlling the DPM model with gain K designed with the MSM model. One observes that the LQR controller designed using the DPM, MSM and the Mix have very similar performance in reducing the angular displacement and damping flexible displacements. The LQR controller designed with DPM model presents a little bit better performance. As result, one can conclude that the controller performance is better when it is designed using the DPM, which means that better model imply in better controller performance.

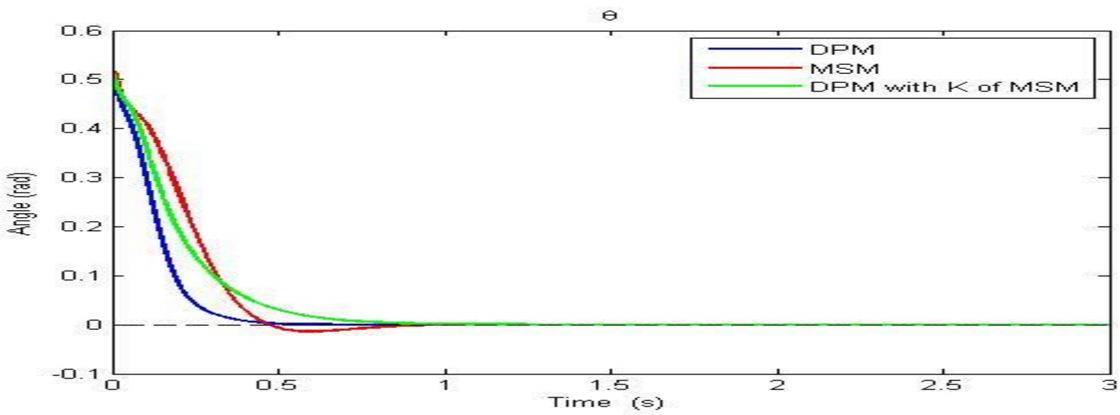

Figure 6 : LQR controller performance reducing angular displacemnet.

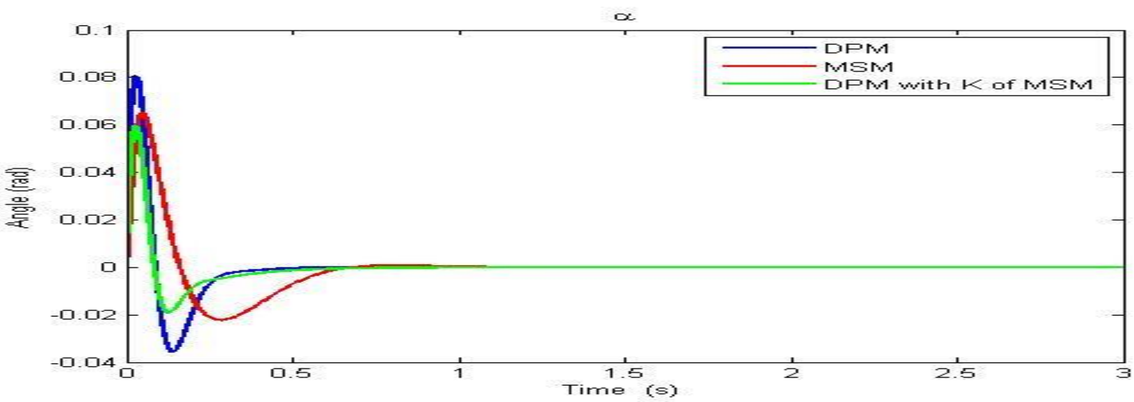

Figure 7 : LQR controller performance damping the flexible displacement.

Figures 8 and 9 shows the LQR controller performance controlling the angular and flexible displacement velocities, when it is designed using the MSM and the DPM models. Figures 8 and 9 also show the LQR Mix controller performance controlling the DPM model with gain K designed with the MSM model. One observes that the LQR controller designed using the DPM, MSM and the Mix have very similar performance in reducing the angular displacement velocity and the flexible displacements velocity. The LQR controller designed with DPM model presents a little bit better performance than the MSM and Mix. Again, one can conclude that the controller performance is better when it is designed using the DPM, which means that better model imply in better controller performance.

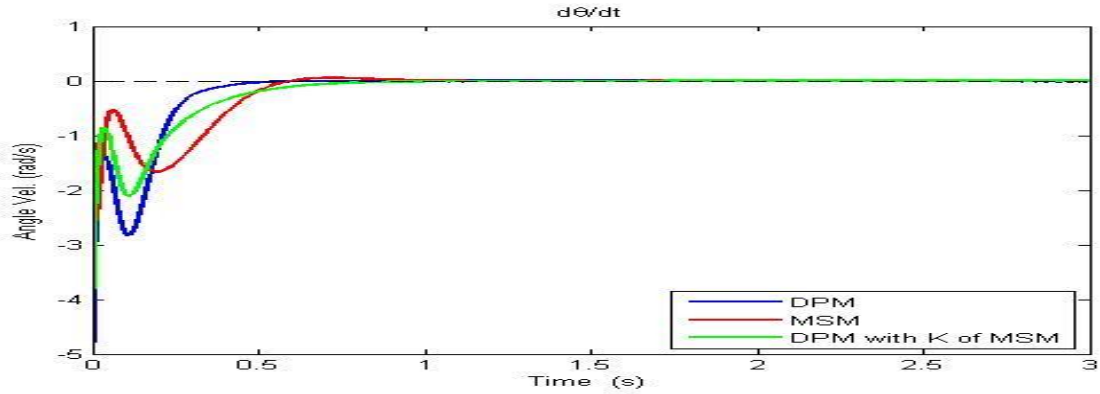

Figure 8 : LQR controller performance reducing angular displacement velocity.

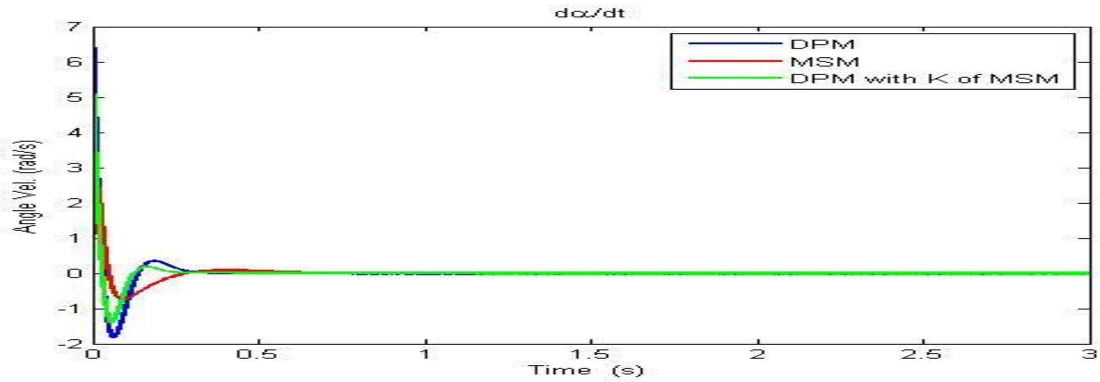

Figure 9 : LQR controller performance damping the flexible displacement velocity.

Figure 10 shows the LQR controller effort to control the rigid-flexibe link . It is possible to see that in the beginning all three controllers spends similar amount of energy and their action finished in less than 0.5 seconds. Finally, one can say that the three LQR controllers are robust since they have good performance even considering the imprecision of the models.

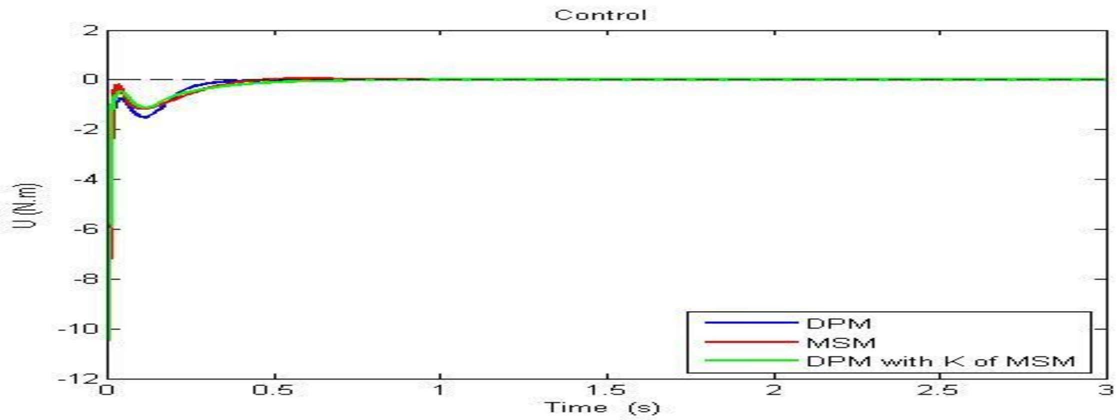

Figure 10 : The energy spends by the three LQR controllers in controlling the rigid-flexible link.

6. CONCLUSIONS

In this paper one investigates and compares the LQR controller robustness and performance when it is designed using two different rigid-flexible beam models which represent the Rotary flexible link module consisting of a rigid central hub connected to a flexible appendage.

The two mathematical models are obtained by the Lagrangian formulation where the first uses a mass-spring model (MSM) configuration to describe the rigid-flexible dynamics and the second applies the Distributed Parameters Model (DPM) method based on the assumed modes method to describe the vibration modes of the system.

The LQR controller designed using the PDM has better performance than the designed using the MSM model. The improvement of performance is related to the fact that PDM represent more faithfully the dynamics of the system. As continuation of this work, one intends to implement the controller experimentally.

7. REFERENCES

Barbosa, E. G. and Góes, L. C. S. Flexible structure control and validation using Flexgage Quanser system. In ABCM. 19th International Congress of Mechanical Engineering. Brasília, DF, Brazil, 2007.

Bigot, P. ; Souza, L. C. G. . Investigation of the State Dependent Riccati Equation (SDRE) Adaptive Control Advantages for Controlling Non-Linear Systems as a Flexible Rotatory Beam. International Journal of Systems Applications, Engineering & Development, v. 8, p. 198-206, 2014.

Conti G.T. and Souza, L.C.G. Satellite attitude control system simulator. Journal of Shock and Vibration. 15, 3-4, (2008), 395-402.

Hall, C.D. , Tsiotras and Shen, H. Tracking Rigid Body Motion Using Thrusters and Momentum Wheels, Journal of the Astronautical Sciences, 2002.

Kaplan M. H, Modern Spacecraft Dynamics and Control, John Wiley & Sons, NY, 1976.

Mainenti-Lopes, I ; Souza, L. C. G. ; Souza, F.L . Design of a nonlinear controller for a rigid-flexible satellite using multi-objective Generalized Extremal Optimization with real codification. Shock and Vibration, v. 19, p. 1-10, 2012.

Pinheiro, E R ; Souza, L C G . Design of the Microsatellite Attitude Control System Using the Mixed Method via LMI Optimization. Mathematical Problems in Engineering (Print), v. 2013, p. 1-8, 2013.

Quanser homepage. at: <http://www.quanser.com/>.

Sales, T.P. ; RADE, D.A. ; SOUZA, L.C.G. . Passive vibration control of flexible spacecraft using shunted piezoelectric transducers. Aerospace Science and Technology (Imprimé), v. 1, p. 12-26, 2013.

Schwartz, J. L.; Peck, M. A. and Hall, C. D. Historical review of air-bearing spacecraft simulators. Journal of Guidance, Control and Dynamics, 26, 4, (2003),513-522.

Souza, A. G. ; Souza, L. C. G. . Design of Satellite Attitude Control System Considering the Interaction between Fuel Slosh and Flexible Dynamics during the System Parameters Estimation. Applied Mechanics and Materials, v. 706, p. 14, 2015.

Souza, L. C. G. ; Control of a Rigid-Flexible Satellite Solar Panel with Non-collocated Sensor/Actuator. Journal of Mechanics Engineering and Automation, v. 5, p. 173-179, 2015.

Souza, L C G ; Souza, A. G. . Satellite Attitude Control System Design considering the Fuel Slosh Dynamics. Shock and Vibration, v. 2014, p. 1-8, 2014.

Souza, A G. ; Souza, L C. G. . Satellite Attitude Control System Design Taking into Account the Fuel Slosh and Flexible Dynamics. Mathematical Problems in Engineering (Print), v. 2014, p. 1-8, 2014.

Souza, L. C. G. ; Victor Arena . Design of Satellite Attitude Control Algorithm Based on the SDRE Method Using Gas Jets and Reaction Wheels. Journal of Engineering, v. 2013, p. 1-8, 2013.

Pinheiro, E R ; Souza, L C G . Design of the Microsatellite Attitude Control System Using the Mixed Method via LMI Optimization. Mathematical Problems in Engineering (Print), v. 2013, p. 1-8, 2013.

Souza, L. C. G. ; Gonzáles, R. G . Application of the State-dependent Riccati Equation and Kalman Filter Techniques to the Design of a Satellite Control System. Shock and Vibration, v. 19, p. 22-28, 2012.

Tsiotras, P. A Spacecraft Simulator for Research and Education. Paper of Georgia Institute of Technology, EUA, 2007.

8. RESPONSIBILITY NOTICE

The authors are solely responsible for the printed material included in this paper.